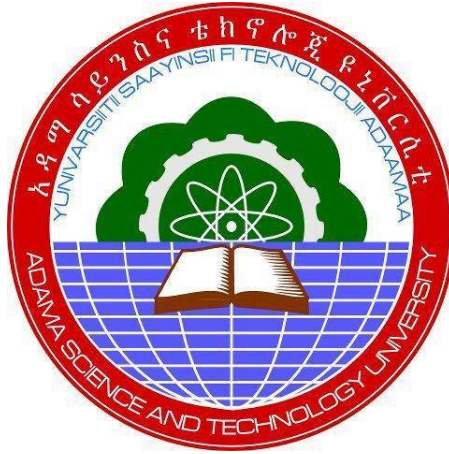


**Numerics of Boundary-Domain Integral Equations for Heat Transfer BVP in
Non-Homogeneous Isotropic Material in Plane**



Dr. Tamirat Temesgen and

Mr. Yadeta Chimdessa

**Final research report submitted to School of Applied Natural Science
Adama Science and Technology University**

**September, 2022
Adama, Ethiopia**

**Numerics of Boundary-Domain Integral Equations for Heat Transfer BVP in
Non-Homogeneous Isotropic Material in Plane**

Dr. Tamirat Temesgen and

Mr. Yadeta Chimdessa

**Final research report submitted to School of Applied Natural Science
Adama Science and Technology University**

**September, 2022
Adama, Ethiopia**

Acknowledgments

The authors would like to thank Adama Science and Technology University for financial support during this research work.

We thank Carlos Fresneda-Portillo, Ph.D., and Nahuel Caruso, Ph.D. for assistance with the code implementations.

Abstract

In this project, we considered heat transfer boundary value problem for non homogeneous isotropic material in a plane. The boundary value problem were reduced to direct united boundary-domain integro differential equation (UBDIDE) and direct segregated boundary-domain integral equation (SBDIE). The mesh-based discretization of the boundary-domain Integral equations with triangular domain elements in conjunction with collocation method were implemented which leads to a system of linear algebraic equation. The resulting algebraic equation were computed. Convergence of the method were investigated. The result shows that both approaches gives good accuracy as the number of nodes increases.

Keywords: Boundary value, Boundary elements, Partial differential equations, Heat equation, Parametrix, integral equations

Contents

1	Introduction	1
1.1	Background of the study	1
1.2	Statement of the problem	2
1.3	Objective of the study	4
1.3.1	General objective	4
1.3.2	Specific objectives	4
1.4	Significant of the study	4
1.5	Scope of the Study	4
2	Literature Review	6
3	Research Methodology	8
3.1	Study procedure	8
4	BVP to its equivalent UBDIDEs/SBDIEs	9
4.1	Boundary Value Problem	9
4.2	Integral Representation in Ω	9
4.3	Discretisation and Approximations	15
5	Numerical Implementation	22
6	Conclusion and recommendation	27
6.1	Discussion and Conclusions	27
6.2	Recommendation	27

List of Tables

Table 5.1	N_{Ω} number of elements, N number of total nodes, N_0 number of internal nodes, and N_S number of boundary nodes	23
Table 5.2	N_{Ω} number of elements, N number of total nodes, N_0 number of internal nodes, and N_S number of boundary nodes, of meshes considered for <i>Example 2</i>	25
Table 5.3	RMS-error and Maximum error for <i>Example 2</i>	26

List of Figures

Figure 5.1	A discretisations for <i>Example 1</i>	23
Figure 5.2	Exact Solution, Absolute Error (UBDIDM), and Absolute Error (SBDIM) for <i>Example 1</i>	24
Figure 5.3	RMS error and Maximum Error vs N_i and N_u	24
Figure 5.4	Domain discretization of <i>Example 2</i>	25

ACRONYMS

BVP	Boundary Value Problem
BIE	Boundary Integral Equation
BDIE	Boundary Domain Integral Equation
BDIDE	Boundary Domain Integro Differential Equation
UBDIDE	United Boundary Domain Integro Differential Equation
SBDIE	Segregated Boundary Domain Integral Equation
BEM	Boundary Element Method
RMS	Root Mean Square

CHAPTER 1

INTRODUCTION

1.1 Background of the study

Mathematical description of many physical processes leads to linear differential and integral equations, or even to integro-differential equation of second order. A reasonably broad class of physical and engineering problems may be reduced to linear second order differential equations. Partial Differential Equations (PDEs) with variable coefficients often arise in mathematical modeling of inhomogeneous media in solid mechanics, electro-magnetics, thermo-conductivity, fluid flow through porous media, and other areas of physics and engineering. Through centuries, different methods of solving such problems have been developed. In any method, it is crucial to investigate the existence and uniqueness of solution, and the well-posedness of the problem or whether the solution depends continuously on a data. In rare cases, one can find the analytical solution for a given boundary value problem. In most engineering and science problems, it is impossible to find the analytical solution for a boundary value problems. In that cases, one has to implement a suitable numerical method to obtain the approximate solution. There are different kinds of transformations that are efficient in analyzing and obtaining solution. One of a classical method to investigate the existence of solution of various boundary value problems (BVP) comprises of reducing the solution of this problem to the solution of an integral equation or a systems of integral equations (Hsiao & MacCamy, 1973; William & McLean, 2000). The method of solving a boundary value problem by transforming to an integral equation or a systems of integral equations is called Boundary Integral Equation method. In short, it is written as, BIE method. Once the boundary integral equation is formulated, one can implement the so called Boundary Element Method (BEM) which requires discretizing only on the boundary of the domain. This will effectively reduces the dimensionality of the problem by one (Brebbia & Dominguez, 1994). This approach is specially preferable for accurate modeling of unbounded domains and well suited for modeling of motion (Brebbia & Dominguez, 1994; Curran et al., 1986; Katsikadelis, 2002; Stephan & Wendland, 1983). The construction of boundary integral equation for a given boundary value problem requires to obtain the fundamental solution of the partial differential equation.

The BIE method has limitation in the sense that a fundamental solution is generally not available, or no applicable method is known to construct it for partial differential equation with *variable coefficients and non-linear problems*. The construction of explicit fundamental solution is possible only for linear differential equation with constant coefficients except in some very special cases. In this case, we can use a parmetrix (Levi function) instead of the fundamental solution in the Green's formula. Here, the boundary value problem is transformed not to boundary integral equation but to *boundary-domain integral equation (BDIE) or boundary-domain integro-differential equation*

(BDIDE), see e.g., (Chkadua et al., 2009a; Mikhailov, 2002) and the references therein, for the corresponding two and three-dimensional boundary value problems.

In the two-dimensional case, the fundamental solution for the formulation of BIE or the parametrix (Levi function) in the formulation of BDIE contains logarithmic function. Because of this, the corresponding potentials have singularities in the domain as well as in the far field. For this reason, the two-dimensional problem should be considered independently. Moreover, in the consideration of boundary value problem in exterior domain, one may work in weighted Sobolev space rather than the ordinary. The appropriate weight function, which insure the unique existence of solution for two-dimensional exterior problem is different from the corresponding three-dimensional exterior problem (Dufera & Mikhailov, 2015).

The boundary element method requires to discretize the boundary of the spatial domain, that leads to the approximation of the boundary geometry. For two dimensional case, where the steady state governing equation has constant coefficient, the boundary elements are just line segments. Similar problems in three dimensions, the boundary elements are either triangular or quadrilaterals. The next step is approximating the unknowns and their normal derivatives on the boundary elements. These can be achieved by linear, quadratic or cubic interpolation polynomials shape functions. The boundary geometry, the unknown quantities and its normal derivatives can be approximated using the same level of interpolation shape functions, called *isoparametric*, see e.g., (Katsikadelis, 2002; Pepper et al., 2014). Inserting these approximation into the integral representations, one can obtain the residuals in different approaches. The *collocation method* is based on requiring the residual to vanishes on certain set of points which are called the collocation points. On the other hand the *Galerkin method* demands the residual to be orthogonal on some set of appropriate test functions, see e.g., (Stefan & Christoph, 2011; Yu et al., 2010) and the reference there in. In this research project we employed the isoparametric interpolation for the approximation of the unknowns and their derivative as well as for the boundary elements. For the residual we implemented the collocation method due to its simplicity (Yu et al., 2010).

1.2 Statement of the problem

Among variety of physical problems that can be solved using the method of integral equation, the heat transfer problem is typical. It is derived from the energy conservation principle and from thermodynamics. Its general form is given as (Carslaw & Jaeger, 1959, Theorem 4.2)

$$-\nabla \cdot \mathbf{q}(x, t) + g(x, t) = \frac{\partial(cu\rho)}{\partial t}, \quad (1.1)$$

where $x = (x_1, x_2, x_3)$ is a point in Ω , t represent time, \mathbf{q} denotes the heat flux, g rate of internal heat generation due to heat sources, ρ material density, c is a specific heat, $u(x, t)$ unknown

temperature, and Ω is domain occupied by the body.

In steady-state heat transfer, that is when the thermal equilibrium has been reached, the temperature distribution within the body does not depend anymore on time and equation (1.1) simplifies to

$$-\nabla \cdot \mathbf{q}(x) + g(x) = 0. \quad (1.2)$$

For two-dimensional problems, the heat may flow in any direction of the x_1x_2 - plane. This flow is described by the *flux vector* \mathbf{q} . According to the generalized Fourier's law, the thermal flux density depends linearly on the gradient of the temperature field and is expressed as

$$\mathbf{q} = -D \cdot \nabla u, \quad (1.3)$$

where

$$D = \begin{bmatrix} a_{x_1x_1} & a_{x_1x_2} \\ a_{x_2x_1} & a_{x_2x_2} \end{bmatrix},$$

is a matrix that provides information about the heat transfer in any direction and it is referred to as the *conductivity matrix*. The negative sign in equation (1.3) is due to the fact the heat flows from higher to lower temperature regions, while the gradient ∇u is directed towards regions of higher temperature. In general D is not a symmetric matrix. However, for the simplicity of the expressions it is assumed here to be symmetric, thus $a_{x_1x_2} = a_{x_2x_1}$. If the material is orthotropic¹, it will be $a_{x_1x_2} = a_{x_2x_1} = 0$. Moreover, we consider the case, $a_{x_1x_1} = a_{x_2x_2} = a(x)$ corresponding to an *isotropic* material and consequently, the equation (1.2) can be written as

$$\sum_{j=1}^2 \frac{\partial}{\partial x_j} \left(a(x) \frac{\partial u}{\partial x_j} \right) = f(x). \quad (1.4)$$

The PDE (1.4) needs to be solved subject to appropriate prescribed boundary conditions.

The numerical implementation of Boundary Integral equation which is called boundary element method is well developed recently. However, obtaining an efficient numerical treatment of boundary value problem with variable coefficient is challenging, because the fundamental solution is not available. The numerical implementation of Boundary domain integral equation for the PDE (1.4) in 3D has been studied in (Grzhibovskis et al., 2013a), with some specific assumptions.

In this project we considered the PDE of the form (1.4) in bounded two dimensional domain

¹In material science and solid mechanics, orthotropic materials have material properties that differ along three mutually-orthogonal twofold axes of rotational symmetry. They are a subset of anisotropic materials, because their properties change when measured from different directions.

where the right hand side function $f(x)$, representing the heat source is form $L_2(\Omega)$ with Dirichlet boundary condition, where the temperature on the boundary is prescribed. In the case of two dimensional problem, the kernel which involves in the integral operator, contains logarithmic function. Such a kernel have additional singularity in the far-field. This creates further challenge for the numerical investigation.

We transformed the boundary value problem to an equivalent boundary-Domain integral equation. Then we implemented numerical technique on the boundary-domain integral equation to simulate the result. We employed the isoparametric interpolation for the approximation of the unknowns and their derivative as well as for the boundary elements. For the residual we implemented the collocation method.

1.3 Objective of the study

This study aimed at achieving the following general and specific objectives.

1.3.1 General objective

The general objectives of this study was to numerically solve (using BEM) the solution of heat transfer BVP in non-homogeneous isotropic material in plane.

1.3.2 Specific objectives

The specific objective of this study were to:

- reduce the BVP for heat equation to an equivalent BDIEs in appropriate Soboleve spaces.
- obtain the Discrete form for the BDIEs.
- study the convergence of the proposed numerical techniques for the problem under study.
- solve heat transfer equation numerically based on boundary element method.

1.4 Significant of the study

The study of this problem have the following importance:

- It contribute a knowledge to the scientific community in the globe and fill the existing gap.
- We believe that the processes of the research have greater contribution in adapting technologies for the future engineering research work in our country, in particular in Macadam Science and Technology University

1.5 Scope of the Study

As boundary-domain integral equation method is relatively recent research area, we gave an emphasis on the implementation of a particular numerical method. We use only the constant

element for the interpolation and the collocation method were implemented for the residual minimization. We considered only smooth domain in a plane and the PDE was limited to linear second order scalar elliptic operator. The study did not considered less regular domains such as, Lipschitz domains. Furthermore, the method did not investigate for higher order elliptic, hyperbolic and parabolic PDEs.

CHAPTER 2

LITERATURE REVIEW

Nowadays, the theory and the application of boundary integral equations are well studied, see e.g., (Constanda, 2020; Costabel, 1988; Hsiao & MacCamy, 1973; Stephan, 1987). One of the most important advantage of this method is that, it reduces a boundary value problem for linear partial differential equation in a domain to an equivalent integral equation on the boundary of the domain. Therefore, it diminishes the problem dimensionality by one, which is very important for construction of various numerical algorithms. The well known numerical method for the approximation of BIE is called Boundary Element Method. This method requires discretizing only the boundary of the domain, which enables one to consider unbounded or exterior problems. This is one of the advantage over the other numerical method like finite difference and finite element method (Atkinson, 1996; Brebbia & Dominguez, 1994; Katsikadelis, 2002).

The transformation of a BVP on a domain to a BIE on the boundary, demands the explicit knowledge of a *fundamental solution* to the original partial differential equation. The use of the fundamental solution in the corresponding Green's formula transforms the BVP to a BIE. The next essential step is to establish the equivalence of the original BVP and the corresponding BIE, and to show the invertibility of the BIE operator, which is crucial for further numerical analysis, see e.g., (Costabel, 1988; Hsiao & MacCamy, 1973; Hsiao & Wendland, 2008).

In (Mikhailov, 2002, 2005, 2006a) localized parametrixes were implemented to reduce a BVP with variable coefficient to a localized BDIE or BDIDE, in (Chkadua et al., 2009a), the parametrix-based direct boundary-domain integral equations for mixed BVPs with variable coefficients has been analyzed. In the work, the equivalence of the BDIEs to the original mixed boundary value problem has been proved and the invertibility of the corresponding operators has been shown for appropriate Sobolev spaces. The same problem has been investigated for exterior domain in (Chkadua et al., 2013).

In (Giroire & Nédélec, 1978), numerical solution of an exterior Neumann problem using a double layer potential has been used. Stephan & Wendland (1983) considered a two dimensional interface problem and derived the corresponding system of boundary integral equation with the direct method. The asymptotic error for the Galerkin approximation of the solution of the integral equation were derived. In (Stephan & Wendland, 1984), the Helmholtz and Laplacian Dirichlet boundary value problems were considered, and boundary integral methods has been implemented to two-dimensional screen and crack problems, a Galerkin scheme on the boundary has been implemented for the numerical solution of the BIE. In (Stephan & Wendland, 1985), the asymptotic

error analysis for boundary element approximation of the the direct BIE for mixed BVP of the Laplacian were addressed. In (Curran et al., 1986) the numerical solution of transient diffusion equation for two-dimensional problem were considered. More numerical implementation of boundary integral equations can be found in (Atkinson, 1996; Brebbia & Dominguez, 1994; Stefan & Christoph, 2011).

We found the formulation of BDIE and BDIDE for the numerical solution of two-dimensional mixed boundary value problem for second order linear elliptic PDE with variable coefficients in (Al-Jawary & Wrobel, 2012) and the author shows that, the method produced accurate results even with coarse meshes. The numerical implementation of Boundary-domain integral equation for the PDE (1.4) in 3D has been studied by Grzhibovskis et al. (2013a). In (Mikhailov & Mohamed, 2012), we found a numerical implementation of a direct united boundary-domain integral equation related to Neumann boundary value problem for a scalar elliptic partial differential equation with a variable coefficient, the corresponding BDIE where discretized with quadrilateral domain elements which leads to a system of linear algebraic equation. The system were solved by LU decomposition and Neumann iterations. Some recent work (Ponzellini Marinelli et al., 2021), presented a stable computation on local boundary-domain integral method for elliptic PDEs. In the paper a new method based on a local integral approach were developed considering local radial bases function interpolations.

CHAPTER 3

RESEARCH METHODOLOGY

For the numerical implementation, mesh-based discretization of the direct UBDIDE and direct SBDIE with collocation method were used. The *collocation method* is based on requiring the residual to vanish on certain set of points which are called the collocation points. The discretization of the spatial domain, that leads to the approximation of the geometry, results in quadrilateral elements. The next step is approximating the unknowns and their normal derivatives on the boundary as well as the domain elements. We have used the linear interpolation polynomials shape functions. The boundary/domain geometry, the unknown quantities and its normal derivatives were approximated using the same level of interpolation shape functions, called *isoparametric*. In this research project we employed the isoparametric interpolation for the approximation of the unknowns and their derivative as well as for the boundary elements.

Generally, the study followed the following procedures.

3.1 Study procedure

To solve the problem under investigation, the following steps were implemented.

- The boundary value problem modeling the heat equation with variable thermal conductivity were transformed to its equivalent direct UBDIDE/SBDIE in the appropriate Sobolev spaces.
- The resulting UBDIDE/SBDIE were discretized using the collocation method;
- The resulting system of linear equations were solved.
- The result were simulated using the FEniCS.

CHAPTER 4

BVP TO ITS EQUIVALENT UBDIDES/SBDIES

4.1 Boundary Value Problem

Let Ω be a bounded domain in a plane, in \mathbb{R}^2 , having piecewise smooth boundary denoted by $\partial\Omega$, $x = (x_1, x_2) \in \mathbb{R}^2$ and $n(x)$ be the exterior unit normal. In our investigation, we assumed that the material has variable thermal conductivity which is space dependent and is given by $a(x)$. That means, it varies with spatial coordinate x . The governing equation for the steady state heat conduction is given by,

$$Au := \sum_{i=1}^2 \frac{\partial}{\partial x_i} \left(a(x) \frac{\partial u}{\partial x_i} \right) = f(x) \quad \text{in } \Omega, \quad (4.1)$$

where the function u is the unknown temperature distribution and f is a given heat distribution in Ω . In order to have a solution, we need boundary condition, i.e., either the temperature, or its flux has to be given on the boundary. In our study we computed the numerical solution where the temperature were known on the boundary and given by,

$$u(x) = \varphi_0(x) \quad \text{on } \partial\Omega. \quad (4.2)$$

The numerical solution were computed in finite subspace of in the space of functions,

$$H^{1,0}(\Omega; A) := \{u \in H^1(\Omega) : Au \in L_2(\Omega)\},$$

where the a function u belongs to $H^1(\Omega)$ implies that $u \in L_2(\Omega)$ and $\nabla u \in L_2(\Omega)$ and the derivative is in distributional sense, see e.g. (Chkadua et al., 2009b; Dufera & Mikhailov, 2015) and the references therein. Moreover, the function f indicating the heat source is in $L_2(\Omega)$ and the boundary condition φ_0 is from $H^{\frac{1}{2}}(\partial\Omega)$ -contains the trace of functions form $H^1(\Omega)$ (Mikhailov, 2011) .

4.2 Integral Representation in Ω

The first step in the boundary integral equation method or boundary element method is to find the integral representation of the boundary value problem. We can write the differential operator A in

the following way,

$$\begin{aligned}
Au(x) &= \sum_{i=1}^2 \frac{\partial}{\partial x_i} \left[a(x) \frac{\partial u(x)}{\partial x_i} \right], \\
&= \sum_{i=1}^2 \frac{\partial a(x)}{\partial x_i} \frac{\partial u(x)}{\partial x_i} + \sum_{i=1}^2 a(x) \frac{\partial^2 u(x)}{\partial x_i^2}, \\
&= \nabla a(x) \cdot \nabla u(x) + a(x) \Delta u(x).
\end{aligned}$$

Multiplying by a test function v , we have

$$vAu = \nabla a(x) \cdot v \nabla u(x) + a(x) v \Delta u(x). \quad (4.3)$$

For the Laplace operator Δ , and functions $u, v \in C^2(\bar{\Omega})$, the following identity holds true;

$$v \Delta u = \nabla \cdot (v \nabla u) - \nabla u \cdot \nabla v. \quad (4.4)$$

Then from the relation (4.4) and (4.3), we have the following,

$$\begin{aligned}
vAu &= \nabla a(x) \cdot v \nabla u(x) + a(x) [\nabla \cdot (v \nabla u) - \nabla u \cdot \nabla v], \\
&= \nabla a(x) \cdot (v \nabla u(x)) + a(x) \nabla \cdot (v \nabla u) - a(x) \nabla u \cdot \nabla v,
\end{aligned}$$

or

$$vAu + a(x) \nabla u \cdot \nabla v = \nabla \cdot (a(x) v \nabla u). \quad (4.5)$$

Now, integrating both side of (4.5) over the domain Ω , applying the divergence theorem, and putting $E(u, v) := a(x) \nabla u \cdot \nabla v$ we obtain, the *first Green's identity*

$$\int_{\Omega} (vAu + E(u, v)) d\Omega = \int_{\Gamma} \gamma^+ v T u(x) d\Gamma(x), \quad (4.6)$$

where γ^+ is the *trace operator* and $T^+ u(x) := a(x) n(x) \cdot \nabla u(x)$, $x \in \partial\Omega$ is the *co-normal derivative operator*, (Chkadua et al., 2009a,c; Mikhailov, 2011).

One of the well known and important relation is the *second Green's identity* which is easily obtained by interchanging the roles of u and v in the first Green's identity (4.6), and subtracting,

$$\int_{\Omega} [vAu - uAv] d\Omega = \int_{\Gamma} \gamma^+ v T^+ u - \gamma^+ u T^+ v] d\Gamma(x). \quad (4.7)$$

A function $P(x, y)$ is said to be the *parametrix* for the partial differential equation (4.1) if it satisfies the equation

$$A_x P(x, y) = \delta(x - y) + R(x, y),$$

where $R(x, y)$ is a remainder. In particular we can show that the function

$$P(x, y) = \frac{\log|x-y|}{2\pi a(y)},$$

is a parametrix and the corresponding remainder is given by

$$\begin{aligned} R(x, y) &= \sum_{i=1}^2 \frac{x_i - y_i}{2\pi a(y)|x-y|^2} \frac{\partial a(x)}{\partial x_i}, \\ &= \frac{1}{2\pi a(y)|x-y|^2} (x-y) \cdot \nabla a(x). \end{aligned}$$

Now taking $u(x)$ as a solution of (4.1) and $v(x)$ as the parametrix $P(x, y)$ in the relation (4.7), we have

$$\int_{\Omega} [PAu - uAP] d\Omega = \int_{\partial\Omega} [PT^+u - uT^+P] d\Gamma(x).$$

Which implies,

$$\begin{aligned} \int_{\Omega} P(x, y) f(x) dx - \int_{\Omega} u(x) [R(x, y) + \delta(x-y)] dx = \\ \int_{\partial\Omega} [P(x, y) T^+ u(x) - u(x) T_x^+ P(x, y)] d\Gamma(x). \end{aligned} \quad (4.8)$$

We know that $u(x) * \delta(x-y) = \int_{\Omega} u(x) \delta(x-y) dx = u(y)$. Hence equation (4.8) becomes,

$$\begin{aligned} u(y) - \int_{\partial\Omega} [\gamma^+ u(x) T_x^+ P(x, y) - \gamma^+ P(x, y) T^+ u(x)] d\Gamma(x) \\ + \int_{\Omega} u(x) R(x, y) dx = \int_{\Omega} P(x, y) f(x) dx \end{aligned} \quad (4.9)$$

Note that, the co-normal derivative of the parametrix $P(x, y)$ is given by,

$$T_x^+ P(x, y) = a(x) \nabla_x P(x, y) \cdot n = \frac{a(x)}{2\pi a(y)} \frac{\cos \phi}{|x-y|}$$

where ϕ is the angle between $(x-y)$ and n . The expression (4.9) is the integral representation of the solution of the differential equation (4.1) at any point $y \in \Omega$ (not on the boundary).

Integral representation on the boundary $\partial\Omega$

Next we see the integral representation of the unknown physical quantity u for points on the boundary $\partial\Omega = \Gamma$. Though our research focuses on smooth domain, we consider the general case where the boundary is not smooth and let y be a corner point on the boundary located at the origin 0. We use the following notations and descriptions,

- Ω^* denotes a sub-domain of Ω obtained by subtracting (cutting out) a small circular section

with center y , radius ε and confined by an arcs say ya and yb , i.e.,

$$\Omega^* = \Omega \setminus B(y, \varepsilon).$$

- Let Γ_ε denotes the arc ab , and n the outward normal to Γ_ε coincides with the radius ε and is directed towards the corner y and α the angle between the tangents of the boundary at the point y ,
- We denote the sum of arcs ay and yb by l , and θ_1 to be the smaller angle formed by one of the tangent line and θ_2 the angle formed by the other tangent line.

We can easily show that; for ε closer to 0, $(\theta_1 - \theta_2) \rightarrow \alpha$, $\Gamma_\varepsilon \rightarrow 0$ and $(\Gamma - l) \rightarrow \Gamma$. Now consider the expression (4.8) on the domain Ω^* , since y lies outside the domain Ω^* , we have $\delta(x - y) = 0$. This implies,

$$\int_{\Omega^*} u(x)\delta(x - y)dx = 0.$$

And hence the equation (4.9) becomes,

$$\begin{aligned} \int_{\partial\Omega^*} [\gamma^+ P(x, y) T^+ u(x) - \gamma^+ u(x) T_x^+ P(x, y)] ds_x \\ + \int_{\Omega^*} u(x) R(x, y) dx = \int_{\Omega^*} P(x, y) f(x) dx. \end{aligned}$$

Since $\partial\Omega^* = (\Gamma - l) \cup \Gamma_\varepsilon$, the above equation becomes,

$$\begin{aligned} \int_{\Gamma - l} [\gamma^+ P(x, y) T^+ u(x) - \gamma^+ u(x) T_x^+ P(x, y)] ds_x \\ + \int_{\Gamma_\varepsilon} [\gamma^+ P(x, y) T^+ u(x) - \gamma^+ u(x) T_x^+ P(x, y)] ds_x \\ + \int_{\Omega^*} u(x) R(x, y) dx = \int_{\Omega^*} P(x, y) f(x) dx. \quad (4.10) \end{aligned}$$

Now taking the limit $\varepsilon \rightarrow 0$, we obtain the following,

$$\begin{aligned} \lim_{\varepsilon \rightarrow 0} \int_{\Gamma - l} [\gamma^+ P(x, y) T^+ u(x) - \gamma^+ u(x) T_x^+ P(x, y)] ds_x \\ = \int_{\Gamma} [\gamma^+ P(x, y) T^+ u(x) - \gamma^+ u(x) T_x^+ P(x, y)] ds_x. \end{aligned}$$

Also,

$$\lim_{\varepsilon \rightarrow 0} \int_{\Omega^*} P(x, y) f(x) dx = \int_{\Omega} P(x, y) f(x) dx,$$

and

$$\lim_{\varepsilon \rightarrow 0} \int_{\Omega^*} u(x) R(x, y) dx = \int_{\Omega} u(x) R(x, y) dx.$$

Next, inserting the parametrization and its conormal derivative,

$$\begin{aligned} \int_{\Gamma_\varepsilon} [\gamma^+ P(x, y) T^+ u(x) - \gamma^+ u(x) T_x^+ P(x, y)] ds_x \\ = \int_{\Gamma_\varepsilon} \frac{1}{2\pi a(y)} \log r \frac{\partial u}{\partial \vec{n}} ds_x - \int_{\Gamma_\varepsilon} u(x) \frac{1}{2\pi a(y)} \frac{\cos \phi}{r} ds_x. \end{aligned}$$

For the circular arc Γ_ε , $r = \varepsilon$, and $\phi = \pi$. Also, $ds_x = \varepsilon(-d\theta)$, because the angle θ is positive in counter-clockwise sense, which is opposite to that of increasing s .

Thus,

$$\begin{aligned} \int_{\Gamma_\varepsilon} \frac{1}{2\pi a(y)} \log r \frac{\partial u}{\partial \vec{n}} ds_x &= \int_{\theta_1}^{\theta_2} \frac{1}{2\pi a(y)} \varepsilon \log \varepsilon \frac{\partial u}{\partial \vec{n}} d(-\theta), \\ &= \frac{1}{2\pi a(y)} \left[\frac{\partial u}{\partial n} \right]_O \varepsilon \log \varepsilon (\theta_1 - \theta_2). \end{aligned} \quad (4.11)$$

The step in (4.11) is due to mean value theorem for integral. When $\varepsilon \rightarrow 0$, the point O of the arc approaches to y . In this case the derivative $\left[\frac{\partial u}{\partial n} \right]_y$, though not defined, it is bounded. Therefore,

$$\lim_{\varepsilon \rightarrow 0} \int_{\Gamma_\varepsilon} \frac{1}{2\pi a(y)} \log r \frac{\partial u}{\partial \vec{n}} ds_x = \frac{1}{2\pi a(y)} \left[\frac{\partial u}{\partial n} \right]_y (\theta_1 - \theta_2) \lim_{\varepsilon \rightarrow 0} \varepsilon \log \varepsilon = 0.$$

Similarly,

$$\begin{aligned} \lim_{\varepsilon \rightarrow 0} - \int_{\Gamma_\varepsilon} u(x) \frac{a(x)}{2\pi a(y)} \frac{\cos \phi}{r} ds_x &= \lim_{\varepsilon \rightarrow 0} - \int_{\theta_1}^{\theta_2} \frac{ua}{2\pi a(y)} \left(\frac{-1}{\varepsilon} \right) \varepsilon d(-\theta) \\ &= \lim_{\varepsilon \rightarrow 0} - \frac{1}{2\pi a(y)} [au]_O (\theta_2 - \theta_1) = \lim_{\varepsilon \rightarrow 0} \frac{\theta_1 - \theta_2}{2\pi a(y)} [au]_O = \frac{\alpha}{2\pi} u(y). \end{aligned}$$

Hence,

$$\lim_{\varepsilon \rightarrow 0} \int_{\Gamma_\varepsilon} [P(x, y) T u(x) - u(x) T_x P(x, y)] ds_x = \frac{\alpha}{2\pi} u(y).$$

Therefore, as $\varepsilon \rightarrow 0$, the expression (4.10) becomes,

$$\begin{aligned} \frac{\alpha}{2\pi} u(y) + \int_{\Gamma} [\gamma^+ P(x, y) T^+ u(x) - \gamma^+ u(x) T_x^+ P(x, y)] ds_x \\ + \int_{\Omega} u(x) R(x, y) dx = \int_{\Omega} P(x, y) f(x) dx. \end{aligned} \quad (4.12)$$

The expression (4.12) is the integral representation of the solution for the differential equation (4.1) at point $y \in \Gamma$, where the boundary is not smooth. For points y , where the boundary is

smooth, $\alpha = \pi$. Hence (4.12)

$$\frac{1}{2}u(y) + \int_{\Gamma} [\gamma^+ P(x,y) T^+ u(x) - \gamma^+ u(x) T_x^+ P(x,y)] d\Gamma(x) + \int_{\Omega} u(x) R(x,y) dx = \int_{\Omega} P(x,y) f(x) dx.$$

Note that, a comparison between (4.9) and (4.12) shows that the function u is discontinuous when the point $y \in \Omega$ approaches to a point to boundary. So we will have a jump condition equal to $(1 - \frac{\alpha}{2\pi})$ for a corner points. And a jump condition equal to $\frac{1}{2}$ for smooth points.

If the point y is located outside the domain Ω , then $\delta(x-y) = 0$ and hence

$$\int_{\Omega} u(x) \delta(x-y) dx = 0.$$

So from equation 4.8,

$$\int_{\partial\Omega} [\gamma^+ P(x,y) T^+ u(x) - \gamma^+ u(x) T_x^+ P(x,y)] d\Gamma(x) + \int_{\Omega} u(x) R(x,y) dx = \int_{\Omega} P(x,y) f(x) dx. \quad (4.13)$$

Equations (4.9), (4.12), and (4.13) can be combined in a single general equation as:

$$c(y)u(y) + \int_{\Gamma} [\gamma^+ P(x,y) T^+ u(x) - \gamma^+ u(x) T_x^+ P(x,y)] dx + \int_{\Omega} u(x) R(x,y) dx = \int_{\Omega} P(x,y) f(x) dx, \quad (4.14)$$

where,

$$c(y) = c(y; \Omega) = \begin{cases} 1, & \text{if } y \in \Omega, \\ 0, & \text{if } y \notin \Omega, \\ \frac{\alpha}{2\pi}, & \text{if } y \in \Gamma. \end{cases}$$

Here α is an interior space angle at a corner point y of the boundary Γ .

The representation (4.13) holds for a function $u \in H^{1,0}(\Omega; A)$. The representation (4.14) is known as direct united boundary-domain integro-differential equation (UBDIDE) (Grzhibovskis et al., 2013a; Mikhailov, 2006b).

If we replace the co-normal derivative $T^+ u$ in the integral representation (4.13) by a new unknown

boundary function say t and applying the equation in domain and its trace on $\partial\Omega$, we get,

$$c(y)u(y) + \int_{\Gamma} [\gamma^+ P(x,y)t(x) - \gamma^+ u(x)T_x^+ P(x,y)] dx + \int_{\Omega} u(x)R(x,y)dx = \int_{\Omega} P(x,y)f(x)dx, \quad (4.15)$$

where $c(y)$ is described above. The integral equation (4.15) is known as the direct segregated boundary-domain integral equation (SBDIE).

4.3 Discretisation and Approximations

Let the domain Ω be partitioned into, say, N_{Ω} linear triangular elements denoted by Ω^e , $e = 1, \dots, N_{\Omega}$, then,

$$\Omega = \bigcup_{e=1}^{N_{\Omega}} \overline{\Omega^e}.$$

Moreover, the intersection $\Omega^i \cap \Omega^j$ for $i \neq j$ must be either empty, common edge or common vertex. We have, say, N total number of vertices of the triangles called nodes denoted by $\{x_A = (x_A, y_A)\}_{A=1}^N$ in $\Omega \cup \partial\Omega$. To each triangular element we associate three vertices from the list x_1, \dots, x_N which can be identified by their indices in this list. Denote the vertices of the element Ω^e by x_a^e , $a = 1, 2, 3$.

Let l_k be a segment formed by two consecutive nodes residing on the boundary, $\partial\Omega$. That is l_k is a segment having the end points $z_k, z_{k+1} \in \partial\Omega$. Then,

$$\partial\Omega = \bigcup_{k=1}^{N_S} l_k.$$

Basis functions

Let us take a triangular reference element (parent domain) in $\xi\eta$ -coordinates denoted by $\Omega^e = \{(\xi, \eta) : 0 \leq \xi \leq 1, 0 \leq \eta \leq \xi\}$ with local nodes given by $\xi_1 = (0, 0)$, $\xi_2 = (1, 0)$ and $\xi_3 = (0, 1)$. We define a one-to-one mapping between the parent domain and the global domain. This mapping is described by,

$$x = x(\xi, \eta), y = y(\xi, \eta).$$

Recall that using chain rule, we have,

$$\begin{bmatrix} dx \\ dy \end{bmatrix} = \begin{bmatrix} \frac{\partial x}{\partial \xi} & \frac{\partial x}{\partial \eta} \\ \frac{\partial y}{\partial \xi} & \frac{\partial y}{\partial \eta} \end{bmatrix} \begin{bmatrix} d\xi \\ d\eta \end{bmatrix}. \quad (4.16)$$

The matrix

$$J := \begin{bmatrix} \frac{\partial x}{\partial \xi} & \frac{\partial x}{\partial \eta} \\ \frac{\partial y}{\partial \xi} & \frac{\partial y}{\partial \eta} \end{bmatrix},$$

is Jacobian matrix. For any given value of $d\xi$ and $d\eta$, (4.16) implies dx and dy are uniquely determined. If we know dx and dy , provided that $\det J \neq 0$, we have

$$\begin{bmatrix} d\xi \\ d\eta \end{bmatrix} = J^{-1} \begin{bmatrix} dx \\ dy \end{bmatrix}.$$

So, if we assume $\det J > 0$, there exist a one-to-one relation between the values $d\xi, d\eta$ and dx, dy , i.e., the mapping is unique, at least locally.

The *local basis functions* on the parent domain, denoted by, N_a^e , $a = 1, 2, 3$ are given as follows,

$$\begin{aligned} N_1^e(\xi, \eta) &= 1 - \xi - \eta, & N_2^e(\xi, \eta) &= \xi, \\ N_3^e(\xi, \eta) &= \eta. \end{aligned}$$

For a point (x^e, y^e) in arbitrary triangular element Ω^e with vertices (x_a^e, y_a^e) , $a = 1, 2, 3$, we defined the mapping by the interpolation,

$$x^e = N_1^e(\xi, \eta)x_1^e + N_2^e(\xi, \eta)x_2^e + N_3^e(\xi, \eta)x_3^e, \quad (4.17)$$

$$y^e = N_1^e(\xi, \eta)y_1^e + N_2^e(\xi, \eta)y_2^e + N_3^e(\xi, \eta)y_3^e. \quad (4.18)$$

To write (4.17)-(4.18) in matrix form, we define

$$\begin{aligned} N^e(\xi, \eta) &= \begin{bmatrix} N_1^e(\xi, \eta) & N_2^e(\xi, \eta) & N_3^e(\xi, \eta) \end{bmatrix}; \\ x^e &= \begin{bmatrix} x_1^e & x_2^e & x_3^e \end{bmatrix}^T, y^e = \begin{bmatrix} y_1^e & y_2^e & y_3^e \end{bmatrix}^T. \end{aligned}$$

Then ,

$$x^e = N^e(\xi, \eta)x^e; \quad y^e = N^e(\xi, \eta)y^e. \quad (4.19)$$

Observe that, this element shape functions possess the needed properties,

$$N_a^e(\xi_b) = \delta_{ab}, \text{ and } \sum_{a=1}^3 N_a = 1.$$

It follows that,

$$x^e(\xi_b) = \sum_{a=1}^3 N_a^e(\xi_b)x_a^e = x_b^e, \quad y^e(\xi_b) = \sum_{a=1}^3 N_a^e(\xi_b)y_a^e = y_b^e.$$

That is, each corner point in the parent domain is mapped to a corner point of the reference element.

Global basis functions: we will denote the global basis function by N_A , $A = 1, \dots, N$, and defined on element e , in terms of the local basis functions given by;

$$N_A(x^e(\xi)) = \begin{cases} N_a^e(\xi(x)), & \text{if } x_A = x_a^e, a = 1, 2, 3, \\ 0, & \text{if } x_A \neq x_a^e, a = 1, 2, 3, \end{cases} \quad (4.20)$$

where $\xi(x)$ are the function inverse to $x(\xi)$ given by the isoparametric mapping. The global basis functions satisfy the δ -property $N_A(x_B) = \delta_{AB}$.

Approximation of the unknown

We use the continuous, piecewise linear basis function for the interpolation of the unknown temperature $u(x) \approx u^h(x)$,

$$u^h(x) = \sum_{A=1}^N N_A(x)u_A, \quad x \in \Omega \cup \Gamma.$$

Here $u(x_A) := u_A$ is the nodal values of the unknown u at the nodes, $A = 1, \dots, N$.

Let us classify the nodes in to two groups, interior nodes having total number N_0 and boundary nodes having total number N_S . Hence, $N_S = N - N_0$.

Similar to [Grzhibovskis et al. \(2013a\)](#) for the 3d case, we assume the global node numbering starts from the interior, then using the Dirichlet boundary condition $u = \bar{u}$ on $\partial\Omega$ we have the following,

$$u^h = \sum_{A=1}^{N_0} N_A(x)u_A + \sum_{A=N_0+1}^N N_A(x)\bar{u}_A, \quad (4.21)$$

where the values \bar{u}_A for $A = N_0 + 1, \dots, N$ are known from boundary conditions.

The discretized co-normal derivative

Let n_k be the outer normal unit vector to the segment l_k and Ω_{l_k} denotes the triangular element which possesses the segment l_k as one of its side. The temperature gradient is approximated by

the gradient of u^h . Hence, the conormal derivative is approximated as follows,

$$\begin{aligned}
T^+u(x) &\approx \gamma^+ a(x)n(x) \cdot \nabla u^h(x), \\
&= \gamma^+ \left(a(x) \sum_{A=1}^N n(x) \cdot \nabla N_A(x) u_A \right), \\
&= a(x) \sum_{A: x_A \in \Omega_{l_k}} n_k(x) \cdot \nabla N_A(x) u_A, \\
&= a(x) \sum_{A=1}^N T_{kA}^\Delta u_A, \quad x \in l_k,
\end{aligned} \tag{4.22}$$

where,

$$T_{kA}^\Delta = \begin{cases} n_k \cdot \nabla N_A, & \text{if } x_A \in \Omega_{l_k} \\ 0, & \text{if } x_A \notin \Omega_{l_k}. \end{cases}$$

Discretized integral representation

Now applying the Green's representation formula (4.14), collocating at the interior nodes x_B , $B = 1, \dots, N_0$, we have,

$$\begin{aligned}
u(x_B) + \sum_{k=1}^{N_S} \int_{l_k} P(x, x_B) T^+ u(x) d\Gamma(x) + \int_{\Omega} R(x, x_B) u(x) dx \\
= \sum_{k=1}^{N_S} \int_{l_k} u(x) T_x^+ P(x, x_B) d\Gamma(x) + \int_{\Omega} P(x, x_B) f(x) dx.
\end{aligned}$$

Substituting (4.21) and (4.22), we have

$$\begin{aligned}
u(x_B) + \sum_{k=1}^{N_S} \int_{l_k} P(x, x_B) a(x) \sum_{A=1}^N T_{kA}^\Delta u_A d\Gamma(x) \\
+ \int_{\Omega} R(x, x_B) \left[\sum_{A=1}^{N_0} u_A N_A(x) + \sum_{A=N_0+1}^N \bar{u}_A N_A(x) \right] dx \\
= \sum_{k=1}^{N_S} \int_{l_k} \sum_{A=N_0+1}^N \bar{u}_A N_A T^+ P(x, x_B) d\Gamma(x) + \int_{\Omega} P(x, x_B) f(x) dx.
\end{aligned}$$

Now shifting the known values to the right hand side and rearranging, we obtain

$$\begin{aligned}
u_B + \sum_{A=1}^{N_0} \left[\sum_{k=1}^{N_S} \int_{l_k} P(x, x_B) a(x) T_{kA}^\Delta d\Gamma(x) \right] u_A + \sum_{A=1}^{N_0} \left[\int_{\Omega} R(x, x_B) N_B(x) dx \right] u_A \\
= \sum_{A=N_0+1}^N \left[\int_{\Gamma} T^+ P(x, x_B) N_A(x) d\Gamma(x) - \sum_{k=1}^{N_S} \int_{l_k} P(x, x_B) a(x) T_{kA}^\Delta d\Gamma(x) \right] \bar{u}_A \\
- \sum_{A=N_0+1}^N \left[\int_{\Omega} R(x, x_B) N_A(x) dx \right] \bar{u}_A + \int_{\Omega} P(x, x_B) f(x) dx.
\end{aligned}$$

We use the following notations, the matrix $\mathbf{V}^a \in \mathbb{R}^{N_0 \times N_S}$, $\mathbf{R} \in \mathbb{R}^{N_0 \times N}$, $\mathbf{K} \in \mathbb{R}^{N_0 \times N}$,

$$\mathbf{V}_{Bk}^a := \int_{l_k} P(x, x_B) a(x) d\Gamma(x), \quad (4.23)$$

$$\mathbf{K}_{BA} := \int_{\Gamma} T_x P(x, x_B) N_A(x) d\Gamma(x), \quad (4.24)$$

$$\mathbf{R}_{BA} := \int_{\Omega} R(x, x_B) N_A(x) dx, \quad (4.25)$$

and the vector $\mathbf{f} \in \mathbb{R}^{N_0}$ can be computed as

$$\mathbf{f}_B = \sum_{e=1}^{N_S} \int_{\Omega^e} P(x, x_B) f(x) dx.$$

Using these notations, we have the following referred to as UBDIDM

$$u_B + \sum_{A=1}^{N_0} \left[\sum_{k=1}^{N_S} \mathbf{V}_{Bk}^a \mathbf{T}_{kA}^\Delta + \mathbf{R}_{BA} \right] u_A = \sum_{A=N_0+1}^{n_{ep}} \left[\mathbf{K}_{BA} - \sum_{k=1}^{N_S} \mathbf{V}_{Bk}^a \mathbf{T}_{kA}^\Delta - \mathbf{R}_{BA} \right] \bar{u}_A + \mathbf{f}_B. \quad (4.26)$$

The SBDIM can be obtained in the same procedure using the segregated boundary in integral equation(4.15).

Domain integral transformation

To compute the matrix entries, we need to transform the integrals from the global domain to the local variables.

$$\begin{aligned}
\mathbf{R}_{BA} &= \int_{\Omega} R(x, x_B) N_A(x) dx, \\
&= \sum_{e=1}^{N_S} \int_{\Omega^e} R(x, x_A) N_A(x) dx, \\
&= \sum_{e=1}^{N_S} \int_0^1 \int_0^1 R(x(\xi, \eta), x_B(\xi, \eta)) N_a^e(\xi, \eta) \det(J) d\xi d\eta.
\end{aligned} \tag{4.27}$$

Also,

$$\begin{aligned}
\mathbf{f}_B &= \sum_{e=1}^{N_S} \int_{\Omega^e} P(x, x_B) f(x) dx, \\
&= \sum_{e=1}^{N_S} \int_0^1 \int_0^1 P(x(\xi, \eta), x_B(\xi, \eta)) f(x(\xi, \eta)) \det(J) d\xi d\eta.
\end{aligned} \tag{4.28}$$

Boundary integral transformation

For the segment l_k formed by two consecutive nodes $z_k = (x_k, y_k)$ and $z_{k+1} = (x_{k+1}, y_{k+1})$, we parameterize it by

$$\begin{aligned}
x &= (1 - \eta)x_k + \eta x_{k+1}, \\
y &= (1 - \eta)y_k + \eta y_{k+1}.
\end{aligned}$$

We will denote by $M_{\alpha}^e(\eta)$, $\alpha = 1, 2$, the local one dimensional basis function that are the traces of the two dimensional basis functions $N_a^e(\xi, \eta)$ and given by,

$$M_1^e(\eta) = (1 - \eta), \quad M_2^e(\eta) = \eta.$$

Now

$$\begin{aligned}\mathbf{V}_{Bk}^a &= \int_{l_k} P(x, x_B) a(x) d\Gamma(x), \\ &= \int_0^1 P(x(\xi, \eta), x_B(\xi, \eta)) a(x(\xi, \eta)) \left[\left(\frac{\partial x}{\partial \eta} \right)^2 + \left(\frac{\partial y}{\partial \eta} \right)^2 \right]^{\frac{1}{2}} d\eta.\end{aligned}\quad (4.29)$$

$$\begin{aligned}\mathbf{K}_{BA} &= \int_{\Gamma} T_x P(x, x_B) N_A(x) d\Gamma(x), \\ &= \sum_{k=1}^{N_S} \int_0^1 T_x P(x(\xi, \eta), x_B(\xi, \eta)) M_A^k(\eta) \left[\left(\frac{\partial x}{\partial \eta} \right)^2 + \left(\frac{\partial y}{\partial \eta} \right)^2 \right]^{\frac{1}{2}} d\eta.\end{aligned}\quad (4.30)$$

Recall that,

$$\begin{aligned}P(x, x_B) &= \frac{\log |x - x_B|}{2\pi a(x_B)} \\ R(x, x_B) &= \frac{1}{2\pi a(x_B) |x - x_B|^2} (x - x_B) \cdot \nabla a(x), \\ T_x^+ P(x, x_B) &= a(x) \nabla_x P(x, x_B) \cdot n = \frac{a(x)}{2\pi a(x_B)} \frac{\cos \phi}{|x - x_B|},\end{aligned}$$

where ϕ is the angle between $(x - x_B)$ and n . The element matrices are usually evaluated using numerical integration techniques, which are selected according to whether the integral is: non-singular, singular or nearly singular. When the collocation point is located away from the element, we obtain non-singular integrals, hence the standard quadrature techniques can be used. When the collocation point is located on the element, the integrals become singular. For accurate numerical integration a variable transformation in the parametric coordinates ξ is needed.

CHAPTER 5

NUMERICAL IMPLEMENTATION

In this section, we implement the numerical experiment. The domain is discretized by conformal triangulations using the mesher tool from (Alnæs et al., 2015).

The accuracy of the method is investigated using two errors which are computed on a set of a fixed N_t nodes: the first is the root mean square (RMS) error given by

$$\epsilon_{RMS}^2 = \frac{\sum_{k=1}^{N_t} (u_k - u_{e,k})^2}{\left(\sum_{k=1}^{N_t} (u_{e,k})\right)^2}, \quad (5.1)$$

and the second is the maximum error given by

$$\epsilon_{max} = \max_{k=1, \dots, N_t} |u_k - u_{e,k}|, \quad (5.2)$$

where u_e is exact solution. The number N_t is different to N_0, N_S and N_Ω and remains the same for all the meshes. We take $N_t \approx 10000$ points uniformly distributed across each mesh.

Example 1

The 3D case of this example is reported by Grzhibovskis et al. (2013b). Considers the original BVP (4.1) defined on a disc of radius $\frac{1}{3}$, $\Omega = B(0, \frac{1}{3}) \subset \mathbb{R}^2$ with no heat source, $f \equiv 0$ and the variable coefficient is given by,

$$a(x, y) = ((x-1)^2 + (y-1)^2)^{-\frac{1}{2}}, \quad (5.3)$$

one can show that the analytical solution is given by;

$$u_e(x, y) = ((x-1)^2 + (y-1)^2)^{\frac{1}{2}}. \quad (5.4)$$

Figure 5.1 depicts a typical discretisation for the given problem.

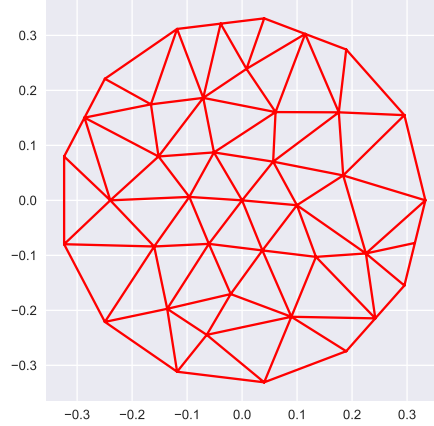


Figure 5.1: A discretisations for *Example 1*

Table 5.1 shows five different meshes denoted by τ_i , $i = 1, \dots, 5$. The total number of elements denoted by N_Ω , N is number of total nodes, while N_0 is number of internal nodes and N_S is the number of nodes on the boundary.

Table 5.1: N_Ω number of elements, N number of total nodes, N_0 number of internal nodes, and N_S number of boundary nodes

Mesh	N_Ω	N	N_0	N_S
τ_1	88	55	34	21
τ_2	135	80	52	28
τ_3	402	233	191	42
τ_4	908	502	221	281
τ_5	1556	823	391	432

Figure 5.2 is the plot for the exact solution and its corresponding error using the two mentioned methods, we observe that the symmetry of the solution and the error distribution across the line $x = y$ for both methods. For the same discretisation τ_3 , the difference between both methods is almost of one order of magnitude.

The root mean square error (ϵ_{RMS}) and maximum error (ϵ_{max}) using different values of the total number of nodes is shown in Figure 5.3. The subplots 5.3a compare the internal nodes (N_i) against errors the two methods. The subplots 5.3b compare the number of the unknowns (N_u) in the final linear system for both cases ($N_u = N_0$ for UBDIDM and $N_u = N_0 + N_S$ for SBDIM). Increasing the number of nodes improves the accuracy of the numerical solution for both methods, but always the SBDIM outperforms the UBDIDM in almost one order of magnitude. There is no relevant difference between errors and N_0 or N_u .

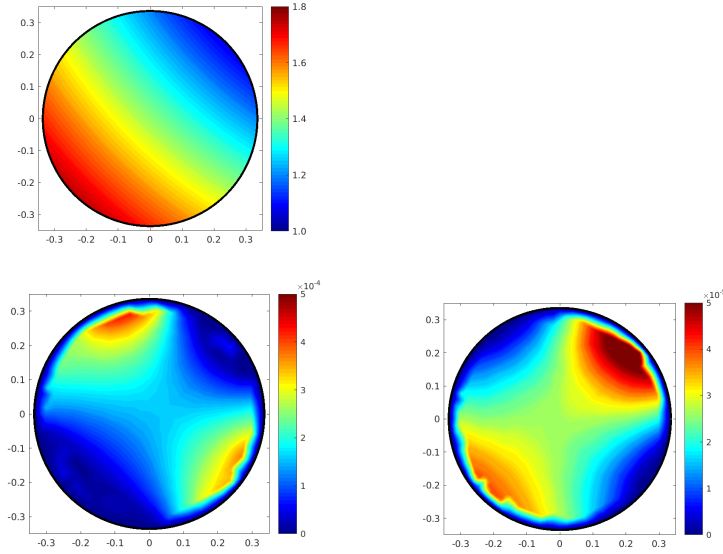
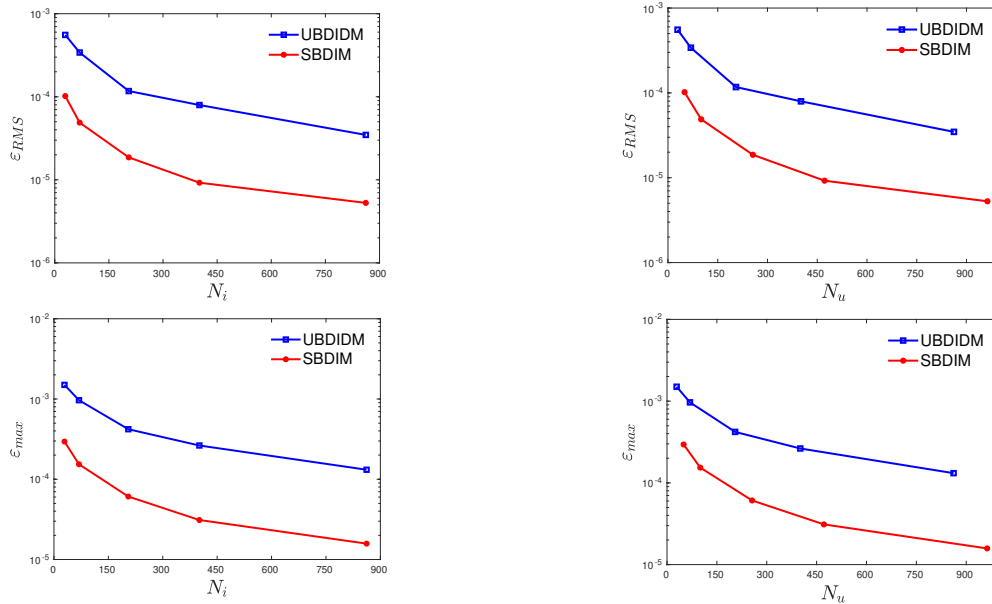


Figure 5.2: Exact Solution, Absolute Error (UBDIDM), and Absolute Error (SBDIM) for Example 1



(a) N_i and N_u

(b) N_i and N_u

Figure 5.3: RMS error and Maximum Error vs N_i and N_u

Example 2

This example is adapted from [Coco & Russo \(2013\)](#), consists of the BVP (4.1) on the domain Ω given by a rotated ellipse centered at the origin (see Figure 5.4), and the boundary is given by parametric equations

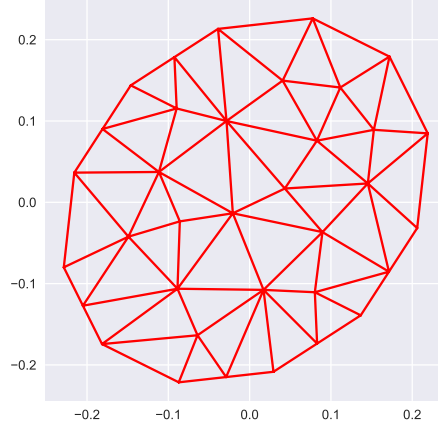


Figure 5.4: Domain discretization of *Example 2*

$$\partial\Omega : \begin{cases} x(t) = \frac{1}{8} \cos(t) - \frac{\sqrt{3}}{10} \sin(t) \\ y(t) = \frac{\sqrt{3}}{8} \cos(t) + \frac{1}{10} \sin(t) \end{cases} \quad t \in [0, 2\pi].$$

In this example the problem has a heat source where the distribution is described by the right-hand side:

$$f(x, y) = e^{(x+y)} (\cos(x+y) - \sin(x+y)) + 2 \sin(x) \cos(y)$$

and variable coefficient representing the heat conductivity of the material is given by; $a(x, y) = 1 + e^{(x+y)}$. The exact solution corresponding to this problem is

$$u_e(x) = \sin(x_1) \cos(x_2). \quad (5.5)$$

As for Example 1, we consider five discretisations (τ_i , $i = 1, \dots, 5$). The structure of this meshes is described in Table 5.2 which gives the values for N_Ω , N , N_0 , and N_S as in the previous problem. For instance, Figure 5.4 shows the domain and its discretisation.

Table 5.2: N_Ω number of elements, N number of total nodes, N_0 number of internal nodes, and N_S number of boundary nodes, of meshes considered for *Example 2*.

Mesh	N_Ω	N	N_0	N_S
τ_1	84	55	33	22
τ_2	152	94	65	29
τ_3	343	197	87	110
τ_4	984	534	384	150
τ_5	2116	1122	921	201

The results of the computational errors are summarized in Table 5.3 where the RMS error and maximum error are shown for each of the five meshes and comparing the *united* method against

Table 5.3: RMS-error and Maximum error for *Example 2*

Mesh	UBDIDM		SBDIM	
	ϵ_{RMS}	ϵ_{max}	ϵ_{RMS}	ϵ_{max}
τ_1	1.50e-03	2.79e-04	1.08e-04	3.05e-05
τ_2	8.44e-04	1.79e-04	5.72e-05	1.71e-05
τ_3	3.80e-04	8.90e-05	2.26e-05	6.81e-06
τ_4	1.65e-04	4.07e-05	9.16e-06	2.86e-06
τ_5	7.86e-05	1.99e-05	4.86e-06	2.68e-06

the *segregated*. From this table, it is clear that as the number of nodes increases, the errors decrease. Once again, the SBDIM overtakes the UBDIDM by one order of magnitude.

CHAPTER 6

CONCLUSION AND RECOMMENDATION

6.1 Discussion and Conclusions

In this research project, we presented two boundary-domain integral formulations for solving steady state heat diffusion with variable heat conductivity in a plane. First, the boundary value problem were transformed to boundary domain integral equations. Following (Grzhibovskis et al., 2013a), we formulated the direct united boundary-domain integro-differential equation (UBDIDE) and the direct segregated boundary-domain integral equation (SBDIE).

Moreover, we included the numerical discretisation of both formulations based on collocation discretisations using continuous and piecewise linear Lagrange elements over triangular meshes of the domain. We analysed the convergence to the solution as the number of elements increases. Last, we provided two numerical examples over different domains. Both methods showed a good accuracy behaviour for different discretisations and in both examples *the SBDIM overcame the UBDIM* in agreement with the results provided in Grzhibovskis et al. (2013b) for the 3D case.

6.2 Recommendation

For the future work we recommend for the investigation of full numerical analysis, such as the theoretical study on convergence, stability and the order of convergence. Since the resulting algebraic equation contains fully populated matrix, there should be a mechanism to obtain sparsely populated stiffness matrix which reduce the computational complexity. Furthermore, extending the study to nonlinear partial differential equations, other kinds of boundary conditions and time-dependent partial differential equation is important. At last, we recommend for the study of full comparison of this method with the finite element, finite difference and other well-known method.

REFERENCES

- Al-Jawary, M., & Wrobel, L. (2012). Numerical solution of the two-dimensional helmholtz equation with variable coefficients by the radial integration boundary integral and integro-differential equation methods. *International Journal of Computer Mathematics*, 89(11), 1463–1487.
- Alnæs, M., Blechta, J., Hake, J., Johansson, A., Kehlet, B., Logg, A., ... Wells, G. N. (2015). The fenics project version 1.5. *Archive of Numerical Software*, 3(100).
- Atkinson, K. E. (1996). *The numerical solution of integral equations of the second kind*.
- Brebbia, C. A., & Dominguez, J. (1994). *Boundary elements: an introductory course*. WIT press.
- Carslaw, H., & Jaeger, J. (1959). *Conduction of heat in solids*. Oxford: Clarendon Press, 1959, 2nd ed., 1.
- Chkadua, O., Mikhailov, S., & Natroshvili, D. (2009a). Analysis of direct boundary-domain integral equations for a mixed bvp with variable coefficient, i: Equivalence and invertibility. *The Journal of Integral Equations and Applications*, 499–543.
- Chkadua, O., Mikhailov, S., & Natroshvili, D. (2009b). Analysis of direct boundary-domain integral equations for a mixed bvp with variable coefficient, i: Equivalence and invertibility. *The Journal of Integral Equations and Applications*, 499–543.
- Chkadua, O., Mikhailov, S., & Natroshvili, D. (2009c). Analysis of some localized boundary-domain integral equations. *Journal of Integral Equations and Applications*, 21(3), 405–445.
- Chkadua, O., Mikhailov, S., & Natroshvili, D. (2013). Analysis of direct segregated boundary-domain integral equations for variable-coefficient mixed bvps in exterior domains. *Analysis and Applications*, 11(4).
- Coco, A., & Russo, G. (2013). Finite-difference ghost-point multigrid methods on cartesian grids for elliptic problems in arbitrary domains. *Journal of Computational Physics*, 241, 464–501. doi: <https://doi.org/10.1016/j.jcp.2012.11.047>
- Constanda, C. (2020). *Direct and indirect boundary integral equation methods*. Chapman and Hall/CRC.
- Costabel, M. (1988). Boundary integral operators on lipschitz domains: elementary results. *SIAM journal on Mathematical Analysis*, 19(3), 613–626.

- Curran, D., Lewis, B., & Cross, M. (1986). A boundary element method for the solution of the transient diffusion equation in two dimensions. *Applied Mathematical Modelling*, 10(2), 107-113. doi: [https://doi.org/10.1016/0307-904X\(86\)90080-6](https://doi.org/10.1016/0307-904X(86)90080-6)
- Dufer, T., & Mikhailov, S. (2015). Analysis of boundary–domain integral equations for variable-coefficient dirichlet bvp in 2d. In *Integral methods in science and engineering* (pp. 163–175). Springer.
- Giroire, J., & Nédélec, J.-C. (1978). Numerical solution of an exterior neumann problem using a double layer potential. *Mathematics of computation*, 32(144), 973–990.
- Grzhibovskis, R., Mikhailov, S., & Rjasanow, S. (2013a). Numerics of boundary-domain integral and integro-differential equations for bvp with variable coefficient in 3d. *Computational Mechanics*, 1–9.
- Grzhibovskis, R., Mikhailov, S., & Rjasanow, S. (2013b). Numerics of boundary-domain integral and integro-differential equations for bvp with variable coefficient in 3d. *Computational Mechanics*, 51. doi: 10.1007/s00466-012-0777-8
- Hsiao, G., & MacCamy, R. (1973). Solution of boundary value problems by integral equations of the first kind. *SIAM review*, 15(4), 687–705.
- Hsiao, G., & Wendland, W. (2008). *Boundary integral equations*. Springer.
- Katsikadelis, J. T. (2002). *Boundary elements: theory and applications*. Elsevier.
- Mikhailov, S. (2002). Localized boundary-domain integral formulations for problems with variable coefficients. *Engineering Analysis with Boundary Elements*, 26(8), 681–690.
- Mikhailov, S. (2005). Localized direct boundary-domain integro-differential formulations for scalar nonlinear bvps with variable coefficients. *Journal of Engineering Mathematics*, 283–300.
- Mikhailov, S. (2006a). Analysis of united boundary-domain integral and integro-differential equations for a mixed bvp with variable coefficients. *Math. Meth. Appl. Sci.*, 29, 715–739.
- Mikhailov, S. (2006b). Analysis of united boundary-domain integro-differential and integral equations for a mixed bvp with variable coefficient. *Mathematical methods in the applied sciences*, 29(6), 715–739.
- Mikhailov, S. (2011). Traces, extensions and co-normal derivatives for elliptic systems on Lipschitz domains. *Journal of Mathematical Analysis and Applications*, 378(1), 324–342.

- Mikhailov, S., & Mohamed, N. A. (2012). Numerical solution and spectrum of boundary-domain integral equation for the Neumann BVP with a variable coefficient. *International Journal of Computer Mathematics*, 89(11), 1488–1503.
- Pepper, D. W., Kassab, A. J., & Divo, E. A. (2014). *An introduction to finite element, boundary element, and meshless methods with applications to heat transfer and fluid flow*. American Society Of Mechanical Engineers.
- Ponzellini Marinelli, L., Caruso, N., & Portapila, M. (2021). A stable computation on local boundary-domain integral method for elliptic PDEs. *Mathematics and Computers in Simulation*, 180, 379–400. doi: <https://doi.org/10.1016/j.matcom.2020.08.027>
- Stefan, A., & Christoph, S. (2011). *Boundary Element Methods*. Springer.
- Stephan, E. (1987). Boundary integral equations for screen problems in \mathbb{R}^3 . *Integral Equations and Operator Theory*, 10(2), 236–257.
- Stephan, E., & Wendland, W. (1983). Boundary element method for membrane and torsion crack problems. *Computer Methods in Applied Mechanics and Engineering*, 36(3), 331–358.
- Stephan, E., & Wendland, W. (1984). An augmented Galerkin procedure for the boundary integral method applied to two-dimensional screen and crack problems. *Applicable Analysis*, 18(3), 183–219.
- Stephan, E., & Wendland, W. (1985). An augmented Galerkin procedure for the boundary integral method applied to mixed boundary value problems. *Applied Numerical Mathematics*, 1(2), 121–143.
- William, & McLean, W. C. H. (2000). *Strongly elliptic systems and boundary integral equations*. Cambridge University Press.
- Yu, K. H., Kadarman, A. H., & Djodjodihardjo, H. (2010). Development and implementation of some BEM variants—a critical review. *Engineering Analysis with Boundary Elements*, 34(10), 884–899.